AGU PUBLICATIONS

Radio Science

RESEARCH ARTICLE
10.1002/2015RS005908

Special Section:
Ionospheric Effects Symposium 2015

Evaluation of the performance of ionospheric models at solar maximum using COSMIC slant TEC measurements

K. F. Dymond[1], C. Coker[1], C. Metzler[1], and S. E. McDonald[1]

[1]Space Science Division, Naval Research Laboratory, Washington, District of Columbia, USA

Key Points:
- Validated several ionospheric models using COSMIC slant total electron content measurements
- Model agreement was reasonable but GAIM data assimilation model showed best performance
- All models showed poorest agreement in the EIA and in the topside ionosphere

Correspondence to:
K. F. Dymond,
kenneth.dymond@nrl.navy.mil

Citation:
Dymond, K. F., C. Coker, C. Metzler, and S. E. McDonald (2017), Evaluation of the performance of ionospheric models at solar maximum using COSMIC slant TEC measurements, *Radio Sci.*, *52*, 378–388, doi:10.1002/2015RS005908.

Received 1 DEC 2015
Accepted 13 FEB 2017
Accepted article online 15 FEB 2017
Published online 14 MAR 2017

Abstract We report the results of a model validation study that assessed how well several ionospheric models captured the slant total electron content, especially at low latitudes near the equatorial ionization anomaly, where horizontal and vertical density gradients are large. We assessed NeQuick, IRI-2007, IRI-2012, SAMI-3, and the Utah State University version of the Global Assimilation of Ionospheric Measurements (GAIM) model. We used slant total electron content measurements made by the Constellation Observing System for Meteorology, Ionosphere, and Climate (COSMIC) constellation during 5 May to 20 June 2012 to test GAIM, NeQuick, IRI-2007, and IRI-2012 and during 1 October 2011 to 31 December 2011 to test SAMI-3, as the SAMI-3 model runs were not available for the 2012 time frame. We found that the GAIM data assimilation model showed the lowest biases, although all of the models typically agreed with the COSMIC measurements to ~8% in the worst case. One area of concern with all of the models was that the mean percentage difference between the COSMIC measurements and the calculated total electron content (TEC) showed significant scatter, >15% at the 1 sigma level; this was attributed to all of the models not capturing the density gradients near the equatorial ionization anomaly (EIA). All of the models underestimated the topside electron density and thus also the ionospheric slab thickness. Since ionospheric models are often validated using near-vertical TEC measurements and the vertical TEC is the product of the electron density at the *F* region peak and the slab thickness, our results suggest that the peak density values in the models may be too high.

1. Introduction

During the past 15 years, data assimilation techniques similar to those used in tropospheric weather forecasting have become important for ionospheric specification and forecasting. These models use a model of the ionosphere, either physics based or empirical, and use a Kalman filter to ingest ionospheric measurements to nudge the model closer to the measurements. This approach has become highly successful with good agreement demonstrated between the assimilative models and validating measurements, especially when the validation measurements come from regions where ample data have been ingested. However, unlike tropospheric weather modeling where millions of measurements are typically assimilated, assimilative modeling of the ionosphere suffers from a lack of measurements. Typically, ionospheric assimilation is driven by near-vertical total electron content (TEC) measurements made by ground-based Global Positioning Satellite (GPS) receivers. While there are thousands of these receivers, they tend to be densely located in some regions of the globe and are relatively sparse in other regions, especially over the open ocean which covers approximately 70% of the Earth's surface.

One of the main concerns with data assimilation using the Kalman filer approach is which model to use. As is well known in the ionospheric community, ionospheric models have their strengths and weaknesses. Empirical models that rely on fitting measurements using functions that are parameterized in terms of local time, day of year, and perhaps solar 10.7 cm flux or other solar activity proxies have been used as the core of data assimilation models [*Yue et al*., 2011a; *Yue et al*., 2012]. Other ionospheric models rely on parameterized basic physics model runs as the core of the data assimilator [*Schunk et al*., 2004; *Scherliess et al*., 2006]. Recently, ionospheric models including a great deal of the physics and chemistry of the ionosphere are being used as the core of assimilation models [*Scherliess et al*., 2009]. Another development is the use of ensemble Kalman filter approaches. The tropospheric weather community uses ensembles of data assimilation models, and this approach is now being considered for ionospheric data assimilation. This model ensemble approach has the advantage of being able to average out the strengths and weaknesses of the models used in the ensemble. In principle, the ensemble Kalman filter approach could be used with semiempirical models like

the International Reference Ionosphere [*Bilitza*, 2001; *Bilitza and Reinisch*, 2008; *Bilitza et al*., 2014]. One of the goals of this study is to assess which models could be used together with Global Assimilation of Ionospheric Measurements (GAIM) as the basis of a multimodel ensemble Kalman filter approach for data assimilation. So if this new paradigm of using a multimodel ensemble Kalman filter approach is to be adopted, the question now arises: how accurately do ionospheric models capture the observed structure of the ionosphere?

This question has been addressed by ionospheric physicists using a variety of ionospheric measurements. Ionospheric models are normally tested against ground-based radar measurements made by ionosondes or incoherent scatter radars, against near-vertical GPS observations of the TEC, against space-based in situ measurements of plasma density and temperature, and vertical incidence TEC measurements made by satellite radar altimeters. While these measurements can assess the local variations in the ionosphere, they cannot adequately decouple the global-scale gradients as functions of altitude, latitude, and longitude. Radio occultation (RO) measurements made by measuring the TEC between the GPS satellites and satellites in low Earth orbit have recently become a popular means of ionospheric specification on a global basis. RO measurements span long lines of sight through the ionosphere and plasmasphere and provide a means of assessing the accuracy of ionospheric models as functions of altitude, latitude, and longitude. One especially unique feature of the RO measurements is the ability to assess vertical gradients. The vertical gradients are important because the altitude structure of the ionosphere is driven by the plasma transport via the equatorial fountain, horizontal winds, and the overall thermodynamic states of the coupled ionosphere/thermosphere system.

In this paper, we present the results of our validation of several ionospheric models against slant TEC measurements made by GPS occultation observed by the Constellation Observing System for Meteorology, Ionosphere, and Climate (COSMIC) satellites [*Anthes et al*., 2008], which are known in Taiwan as FORMOSAT-3. Since late 2006, this six-satellite constellation has had complete coverage in local time and the measurements cover the globe. We focus on the use of the slant TEC as our metric for assessing model accuracy because it provides a means for assessing how well the models predict the vertical structure of the ionosphere.

2. Approach

2.1. Models Tested

In our study, we used COSMIC slant TEC measurements to assess five ionospheric models. We assessed the following ionospheric models: NeQuick, International Reference Ionosphere (IRI)-2007 and IRI-2012, SAMI-3 (Sami is Another Model of the Ionosphere, version 3), and the Utah State University version of the Global Assimilation of Ionospheric Measurements (GAIM) model. We assessed output of the Gauss-Markoff version of the Global Assimilation of Ionospheric Measurements model (GAIM) [*Schunk et al*., 2004; *Scherliess et al*., 2006] to determine how well a data assimilation model specifies the slant TEC. The GAIM model ingested the following ionospheric measurements: ionograms measured by a limited number of ionosondes, near-vertical GPS TEC measurements, in situ data from the Defense Meteorological Satellite Program (DMSP) satellites, and a limited set of COSMIC occultation TEC measurements. The GAIM model produced ionospheric specifications every 15 min on a grid 15° in longitude by 3° in latitude poleward of 70.5° and 4.667° at latitudes equatorward of 70.5° and altitude resolution of 4 km between 92 and 180 km, and 20 km from 180 to 1380 km. The NeQuick, IRI-2007, IRI-2012, and SAMI-3 models were evaluated to determine their accuracy and utility as models for use in a multimodel ensemble Kalman filter data assimilation scheme. To emulate running the IRI-2007 and IRI-2012 [*Bilitza*, 2001; *Bilitza and Reinisch*, 2008; *Bilitza et al*., 2014] models in near-real time and to better capture the day-to-day variation of the solar EUV flux, we used the daily 10.7 cm flux to generate estimates of the daily R_z, the sunspot number, and I_G, the Ionospheric Index; these daily values and the daily 10.7 cm flux were used as inputs to the IRI models. This is a nonstandard method for running IRI, which is most commonly run with 12 month averages of the R_z and I_G to specify the monthly average of the ionospheric state. We used fits to the yearly average of the monthly mean R_z and I_G, provided as part of the IRI distribution, to the monthly mean of the 10.7 cm flux to specify these parameters. The fitting functions (D.P. Drob, private communication, 2012) are

$$R_z = -99.3464 + 1.73449\,F_{10} - 0.00275384\,F_{10}^2$$

$$I_G = -141.638 + 2.37452\,F_{10} - 0.00470850\,F_{10}^2$$

where R_z is the sunspot number, I_G is the Ionospheric Index, and F_{10} is the daily value of the 10.7 cm solar flux in solar flux units (sfu: $10^{-22}\,\mathrm{W\,m^{-2}\,Hz^{-1}}$). The IRI models have a variety of settings allowing for a great

deal of flexibility when they are run. In particular, the models can use either the International Radio Consultative Committee (CCIR) or the International Union of Radio Science (URSI) coefficients in the calculation of the critical frequency of the F_2 ionosphere, f_0F_2, which is used to derive the peak electron density. Except for feeding in the daily indices as noted above, the IRI models were run using the default settings, which select the URSI coefficients. A comparison between IRI-2007 run using the conventional approach and using our approach, driven by the daily 10.7 cm flux, showed minimal impact on the results we present later. We also evaluated NeQuick [*Di Giovanni and Radicella*, 1990; *Radicella and Zhang*, 1995] which is a basic research model developed jointly at the Aeronomy and Radiopropagation Laboratory of the Abdus Salam International Centre for Theoretical Physics (ICTP), Trieste, Italy, and at the Institute for Geophysics, Astrophysics and Meteorology of the University of Graz, Austria. NeQuick is the model that will be used to correct the Galileo (European equivalent to GPS) system geolocations for ionospheric refraction. This model was also run using the daily 10.7 cm solar flux as input; the 2002 release of the code (ITU-R) was used in this study. Like IRI, the NeQuick model uses tabulated coefficients in the calculation of the critical frequency of the F_2 ionosphere, f_0F_2; however, the NeQuick model uses the International Radio Consultative Committee (CCIR) coefficients. The IRI and NeQuick models were run on the GAIM spatial and temporal grids so that interpolation errors were similar between the models. Lastly, we assessed SAMI-3 [*Huba et al*., 2008; *Huba et al*., 2000]. The SAMI-3 model is a first-principles physics model of the ionosphere. For this study, SAMI-3 modeled the plasma and chemical evolution of seven ion species (H^+, He^+, N^+, O^+, $N_2{}^+$, NO^+, and $O_2{}^+$). The complete ion temperature equation was solved for three ion species (H^+, He^+, and O^+) as well as the electron temperature equation. The magnetic field is modeled as a dipole fit to the International Geomagnetic Reference Field (IGRF); the grid is specified over ±60° magnetic latitude. We used SAMI-3 coupled with the Scherliess-Fejer empirical vertical drift model [*Scherliess and Fejer*, 1999]. The thermospheric neutral densities, temperature, and winds were provided by the empirical models NRLMSISE-00 [*Picone et al*., 2002], HWM07 [*Drob et al*., 2008], and DWM07 [*Emmert et al*., 2008]. The daily solar extreme ultraviolet irradiances from 5 to 105 nm were obtained from the NRLSSI model, which is based on measurements made by the Solar Extreme-ultraviolet Experiment (SEE) on the NASA Thermospheric, Ionospheric, and Mesospheric Energy and Dynamics (TIMED) satellite [*Lean et al*., 2011]. More details on the simulations are provided in *McDonald et al*. [2014]. SAMI-3 uses its own nonuniform internal latitude, longitude, altitude, and universal time grids. The SAMI-3 results were interpolated onto uniformly spaced latitude, longitude, and altitude grids that were different from the GAIM grids. However, as discussed below, the integration and interpolations were of sufficiently high quality that this difference was deemed insignificant.

2.2. Data

Routine observations of the Earth's ionosphere are being made by the sensors on the six-satellite Constellation Observing System for Meteorology, Ionosphere, and Climate (COSMIC/FOMOSAT-3, CF3 in this work) launched on 15 April 2006 as a joint venture between the United States and the Republic of China (Taiwan) [*Anthes et al*., 2008]. Each CF3 satellite carries three instruments to study the Earth's ionosphere: the GPS Occultation Experiment (GOX), the Tiny Ionospheric Photometer (TIP), and the Tri-Band Beacon (TBB). The CF3 satellites are a powerful means of studying and specifying the ionosphere from the global scale down to the regional scale using this combination of measurements. The CF3 satellites have had essentially 24 h local time coverage since early 2007, when the constellation became fully deployed. This paper focuses on the GPS occultations observed by the GOX instruments. The GOX instruments often produce more than 2500 ionospheric occultations per day. These occultations are routinely inverted to produce electron density profiles, but those are not of interest in this work. The COSMIC products are freely available on the University Corporation for Atmospheric Research's COSMIC Data Acquisition and Analysis Center (September 2007, http://cosmic-io.cosmic.ucar.edu/cdaac/login/cosmic/, accessed 6 June 2008) website. The COSMIC slant TECs are accurate to ~ 1–3 TECU (total electron content unit, 1 TECU = 10^{16} el m^{-2}) after correction for multipath and other errors [*Yue et al*., 2011b]; we used these processed TECs.

The SAMI-3 and GAIM model outputs were not available for an overlapping time interval, so we used separate time intervals. The GAIM, IRI, and NeQuick models were compared against COSMIC measurements made during the 5 May to 20 June 2012 time period, while the SAMI-3 model was compared against COSMIC measurements made during the 1 October to 31 December 2011 time period. These time intervals had similar geomagnetic and solar conditions and were as close together as was practical, given the availability of the model output. The models were validated against all available COSMIC slant TECs available for a total of

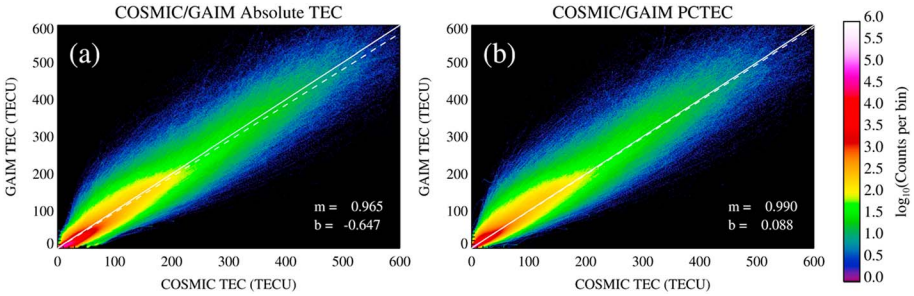

Figure 1. (a) The scatterplot of the GAIM absolute slant TEC versus the COSMIC absolute slant TEC. The solid white line is of unity slope indicating perfect agreement, while the dashed line is the least absolute deviation fit to the data. The slope and intercept of the least absolute deviation line are shown. (b) Same format as Figure 1a but shows the TECs relative to the 0° elevation LOS in each occultation. Note that the slope is closer to 1, and the magnitude of the intercept is now smaller, meaning that the biases in Figure 1a are partly due to the plasmasphere.

44,872 occultations, during the 5 May to 20 June 2012 time period, and 99,941 occultations, during the 1 October to 31 December 2011 time period. A typical occultation from a satellite in the COSMIC constellation occurs over a time frame of order several hundred seconds. During an occultation, the TEC is typically sampled at a 1 s cadence resulting in several hundred measurements. In this work, we treat each TEC sample as an independent measurement. This resulted in approximately 20,834,046 lines-of-sight (LOS) TEC measurements for the 5 May to 20 June 2012 time period and 34,459,872 TEC measurements during the 1 October to 31 December 2011 time period. We used all of the available TEC measurements for our comparison yielding complete local time coverage. We note that the GAIM model ingested some of the TEC measurements we used in our validation. The GAIM model performs its own internal data quality checks so that occultation profiles where there was scintillation were not ingested and occultations with data gaps were also discarded. The TEC measurements obtained using the precise orbit determination receivers on the COSMIC satellites sometimes do not cover the total extent of the ionosphere and hence were not ingested by GAIM; however, we included those in our validation data set. During the 5 May to 20 June 2012 time period of our study, GAIM ingested ~24,000 COSMIC occultations, ~55,000 ionosonde measurements, ~66,000 Special Sensors-Ions, Electrons, and Scintillation (SSIES) in situ densities measured by the DMSP satellites, and ~131,000 ground-based GPS TEC measurements. While there is some overlap between the COSMIC occultation TEC measurements used to validate GAIM and the occultation measurements ingested by GAIM, our TEC validation set used 1.87 times as many occultations as GAIM ingested; thus, the overlap is not complete. Also, since GAIM uses vertical and horizontal correlation lengths to weight-ingested data and thereby mitigate artifacts caused by data assimilation, we wanted to assess the effects of the correlation lengths on the model's performance and therefore used TEC data that were ingested by GAIM as part of the validation. We shall see from the analysis below that GAIM is strongly driven by the more numerous ground-based measurements, most of which come from the Northern Hemisphere.

One major concern for the analysis was the minimization of representation errors caused by the spatial resolution of the model grids and by the LOS integration. To minimize errors due to model spatial resolution and to better intercompare models, all models (with the exception of SAMI-3 which uses its own grids) were run on the GAIM spatial and temporal grids, resulting in similar representation errors between models. Electron density from the models was interpolated onto the LOS using tricubic Catmull-Rom spline interpolators [*Catmull and Rom*, 1974] and integrated using an eighth-order Simpsons' rule quadrature with 101 points along each LOS to minimize integration error.

3. Results and Discussion

Figure 1a shows a scatterplot comparison of the GAIM-derived absolute TEC to the measured COSMIC absolute TEC presented as a two-dimensional histogram. To capture the large dynamic range present in the histogram, the common logarithm of the frequency of occurrence is shown. This format tends to overemphasize the outlier population that has low frequency of occurrence. The solid white line is of unity slope indicating perfect agreement between the measurements, while the dashed white line is the trend line derived by

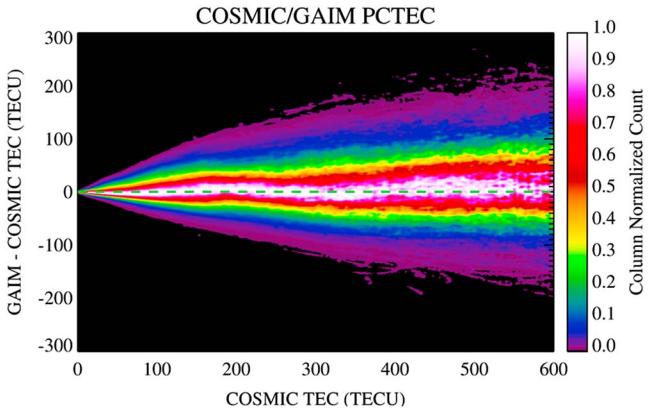

Figure 2. The scatterplot from Figure 1b rotated clockwise by 45° and normalized to the peak count at a fixed COSMIC TEC (column normalized). The dashed green line indicates the line of perfect agreement.

performing a least absolute deviation of a linear function to the histogram. There is a high degree of correlation between the GAIM and COSMIC TECs; however, the GAIM cluster has a slope of 0.97, so that GAIM is underestimating the TEC, on average, by about 3%. There is also a −0.6 TECU additive bias (*y* intercept); this bias likely represents additional plasma in the plasmasphere that is not accounted for in GAIM but which is present in the COSMIC measurements. We approximately remove this bias by subtracting the TEC from the 0° elevation (this is measured with respect to the COSMIC satellite's local horizon) LOS in each occultation from the remainder of the lines of sight in the occultation to produce the plasmasphere-corrected TEC (PCTEC); this correction was applied to both the COSMIC and modeled TECs. Figure 1b shows the PCTEC comparison between GAIM and COSMIC. Our approximate correction has removed the additive TEC bias and improved the overall agreement between the data sets. GAIM is now seen to be underestimating the PCTEC by only about 1%. Note that this comparison covers all local times, and 47 days of time, as well as all longitudes and latitudes. The agreement indicates that GAIM does an excellent job of ionospheric specification, on average.

The problematic feature evident in both Figures 1a and 1b is the scatter of the TEC measurements. This indicates that there are occasions when GAIM is off the mark. Since the trend line fit to the 2-D histogram is ~1, we can subtract the COSMIC TEC from the GAIM TEC and derive the distribution function shown in Figure 2. If we now take vertical cuts across this distribution (Figure 3), we can see how the scatter varies as a function of the TEC. The half width at half maximum (HWHM) scatter of the GAIM TEC with respect to the measurements is ~ 15-20%, for TECs < ~200 TECU. The scatter is ~5–10% at TECs > 200 TECU, independent of the TEC value. While this scatter is most likely due to space weather that is not captured by the GAIM model, we first investigate other possible causes of the scatter.

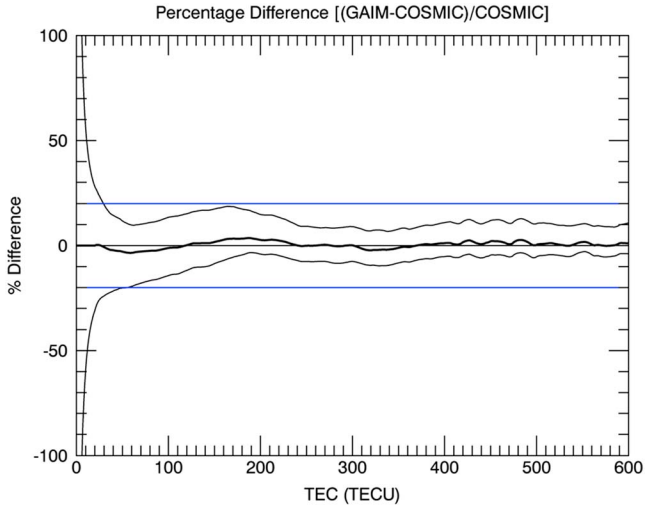

Figure 3. The percentage difference plot derived from the scatterplot in Figure 2. The solid black line indicates the mode of the distribution at each column across the image. The thinner black lines indicate the upper standard deviation and the lower standard deviation, as the distributions are asymmetric, while the blue horizontal lines indicate 20% difference. The GAIM model produces an accurate representation of the ionosphere, on average.

We next examined three possible causes for the scatter: geomagnetic and solar variability driving space weather, model resolution, and data availability for ingestion. To determine whether the scatter was due to geomagnetic and solar activity, we produced daily 2-D histograms, like those in Figure 1b, and fit trend lines to the histograms. Figure 4a shows the variability of the daily trend line slopes; Figure 4b shows the 10.7 cm solar flux in solar flux units (10^{-22} W cm^{-2} s^{-1} Hz^{-1}) and the *ap* index in nanoteslas. There is no obvious correlation related to either geomagnetic or solar drivers; we thus conclude that the scatter is not due solely to geomagnetic or solar activity, although there is likely some contribution from these two sources.

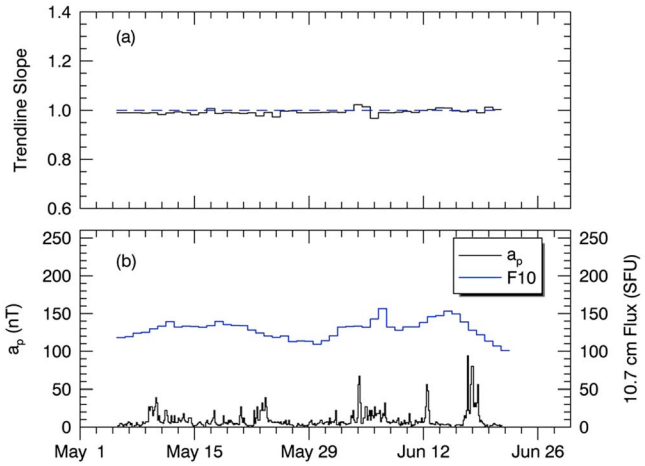

Figure 4. (a) The best fit trend line slope to the PCTEC as a function of time during 2012, with the dashed line indicating a slope of unity. (b) The 10.7 cm flux (SFU) and the *ap* index in nanoteslas over the same time interval as Figure 4a. The trend line slope shows some day-to-day variability, but there is no evident correlation with either solar extreme ultraviolet or geomagnetic variability.

Next, we examine the effects of model resolution. We randomly selected 10,000 LOS from 1 day's worth of COSMIC occultations. For each LOS, we used 101 equally spaced points and calculated the latitudes, altitudes, and longitudes at those points. Then, at a fixed time and date, we calculated the electron density at these points using our interpolation scheme and using the IRI-2007 model run at the GAIM spatial resolution. We also calculated the TEC using IRI-2007 run for each point along the LOS. The LOS TECs were calculated from each set of electron densities. We calculated the percentage difference between the TEC calculated by interpolation and TEC calculated by direct evaluation of IRI-2007. This was then histogrammed and is shown in Figure 5. The GAIM spatial resolution was ruled out as a cause for the scatter, as the mean difference between the two calculations was ~ −0.04% with a standard deviation of 0.4%.

Lastly, we examine the effect of data availability. We note that GAIM is largely driven by ground-based GPS TEC and that most of those measurements are from North America, Europe, Australia, and Japan. For this analysis and in subsequent analyses below, we study the model performance as functions of longitude, latitude, and altitude by geolocating the slant TEC to the tangent ray height of the measurement. This approach is commonly used in the interpretation of limb sounding data, and we adopt it here. We calculated the percentage difference between the COSMIC and GAIM TECs and binned this in latitude and longitude to produce a map. To help suppress the presence of the large outliers evident in Figure 1 and to make the map more consistent with the plot in Figure 3, we calculated the mean and standard deviation of the distribution and selected values that fell within the 90% confidence interval, $\pm 1.65\sigma$ of the mean. Figure 6 shows a map of the mean percentage difference between the COSMIC and GAIM TECs confirming that much of the scatter comes from regions where there is no ground-based TEC data to drive the model, such as in the Southern Hemisphere or over open ocean. Additionally, the region of the equatorial ionization anomaly is another region where the GAIM and COSMIC disagree. The equatorial ionization anomaly (EIA) region is caused by the equatorial fountain that lifts plasma upward where it then drifts poleward along the magnetic field lines. The dynamics of this region are difficult to capture without vertical ion drift measurements which were not available for ingestion, so it is not surprising that GAIM has difficulty capturing this dynamic region.

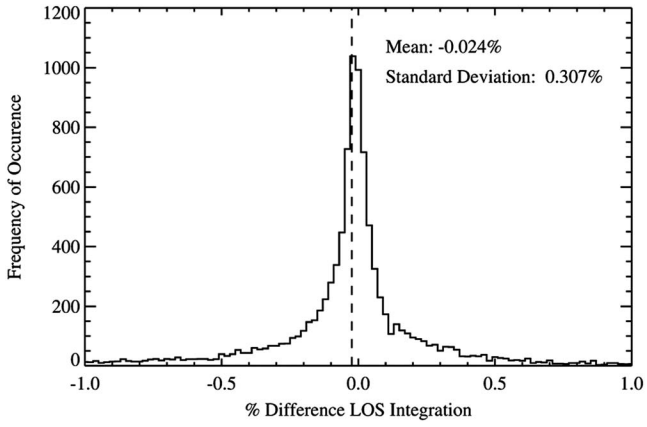

Figure 5. Percentage difference between line-of-sight integrations through an IRI-2007 ionosphere using interpolation of IRI run at the GAIM resolution compared to integrations using IRI run at the actual line-of-sight points.

Before we proceed to comparing the other models to the COSMIC TEC, we need to discuss the SAMI-3 data. SAMI-3 model runs were not available during the time interval used for the testing of the other models, so we opted to use model runs that

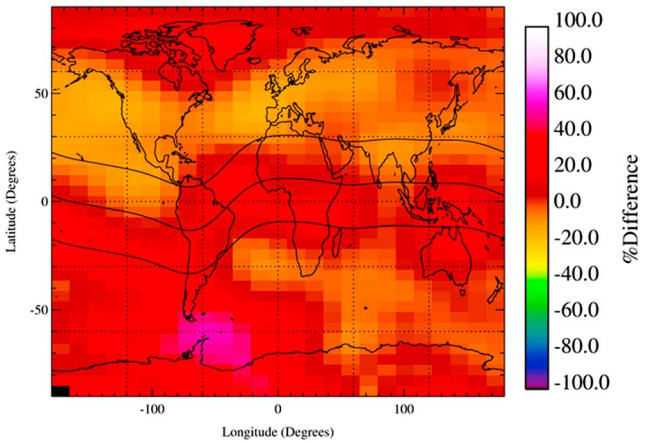

Figure 6. The mean percentage difference between the GAIM TEC and the COSMIC TEC. This average is over all local times and over the 47 day period. Note that the largest errors are near the magnetic equator (black curve) and in the South Atlantic Ocean but that over much of the globe the ratio lies between −0.2 and 0.2, consistent with the percentage difference plot shown in Figure 3. The region of the equatorial ionization anomaly lies mostly over open ocean where there are few data sources to drive the GAIM model.

were close to our study interval. The time interval chosen for the SAMI-3 comparison is 1 October to 31 December 2011. Similar to Figure 4, Figure 7a shows the variability of the daily trend line slopes for SAMI-3; Figure 7b shows the 10.7 cm solar flux in solar flux units (10^{-22} W cm^{-2} s^{-1} Hz^{-1}) and the *ap* index in nanoteslas. As in the GAIM study case, there is no obvious correlation related to either geomagnetic or solar drivers; we thus conclude that the scatter in the SAMI-3 plots is not due solely to geomagnetic or solar activity, although there is likely some contribution from these two sources. Additionally, the solar flux and geomagnetic activities are similar in the two time periods used in the study, so we included the SAMI-3 results into our study.

Next, we intercompare the performance of the other models. Figure 8 shows scatterplots of the TECs derived by integration through the other models versus the COSMIC TECs; note that we are presenting PCTEC, as our focus is solely on ionospheric specification. While the IRI models and NeQuick do not have plasmaspheric contributions, the GAIM, SAMI-3, and COSMIC TECs do contain plasmaspheric contributions. To make the comparisons as fair as possible, we treated the slant TECs from COSMIC and the models in a consistent way by subtracting off the 0° elevation line of sight from the TECs in an occultation to produce the PCTEC. As noted earlier, the GAIM model shows excellent performance, within 1% of the COSMIC PCTEC. SAMI-3 performs fairly well, underestimating the TEC on average by about 1%; however, the scatter is large. The climatology models, IRI-2007, IRI-2012, and NeQuick underestimate the TEC by 8%, 8%, and 6%, respectively. The agreement of the climatology models might be improved by tuning the input drivers to minimize the TEC error. Figure 9 shows the percentage difference plots analogous to Figure 2. Note that all of the models exhibit larger scatter than GAIM, although the scatter of the NeQuick model approaches that of GAIM at TECs > 300 TECU.

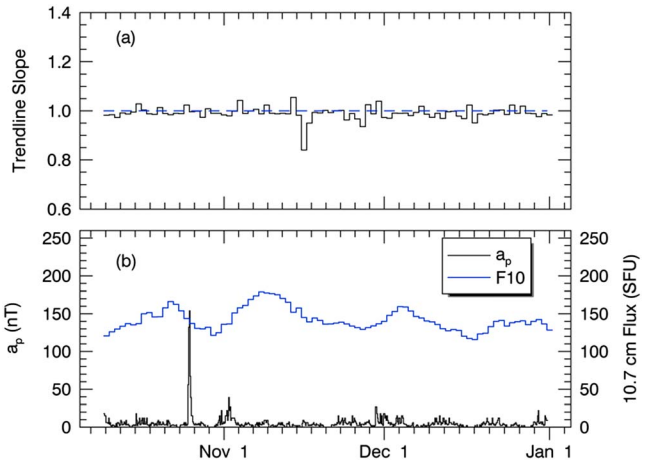

Figure 7. (a) The SAMI-3 best fit trend line slope to the PCTEC as a function of time in late 2011, with the dashed line indicating a slope of unity. (b) The 10.7 cm flux (SFU) and the *ap* index in nanoteslas over the same time interval as Figure 7a. The trend line slope shows some day-to-day variability, but there is no evident correlation with either solar extreme ultraviolet or geomagnetic variability.

One of the key points of this study was to characterize the performance of the models as functions of latitude, longitude, and altitude. To perform this type of comparison, we assume that the PCTEC can be geolocated at the location of the tangent ray height. We recognize that this approach is imperfect, especially in regions of high gradient, but it is commonly used and so we adopt it here. Figure 10

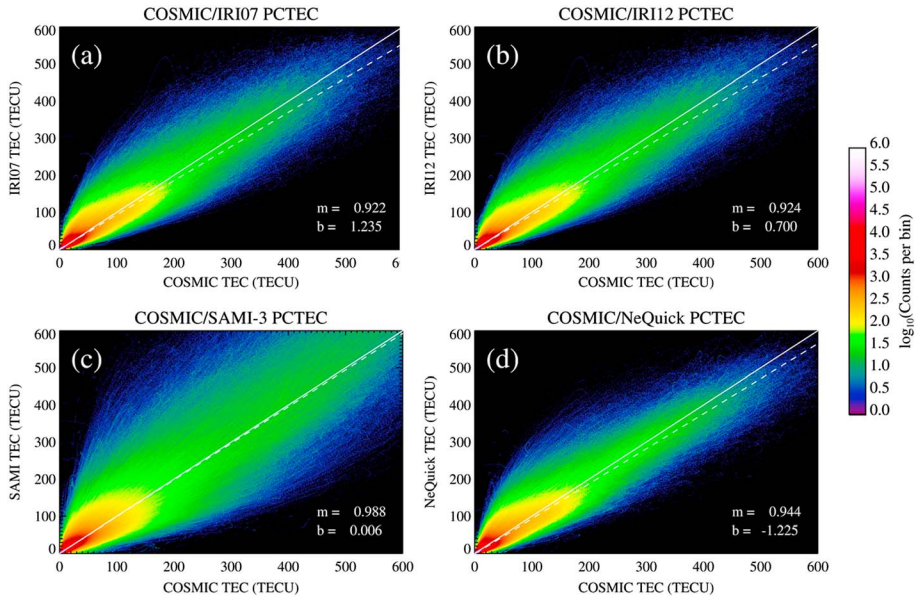

Figure 8. Scatterplots of the PCTECs derived from the other models versus the COSMIC PCTECs: (a) IRI-2007, (b) IRI-2012, (c) SAMI-3, and (d) NeQuick. The SAMI-3 model underestimated the TEC by ~1%, while IRI-2007, IRI-2012, and NeQuick underestimated the TEC by 8%, 8%, and 6%, respectively. The underestimation might be reduced by tuning the geomagnetic and solar parameters used to drive the models.

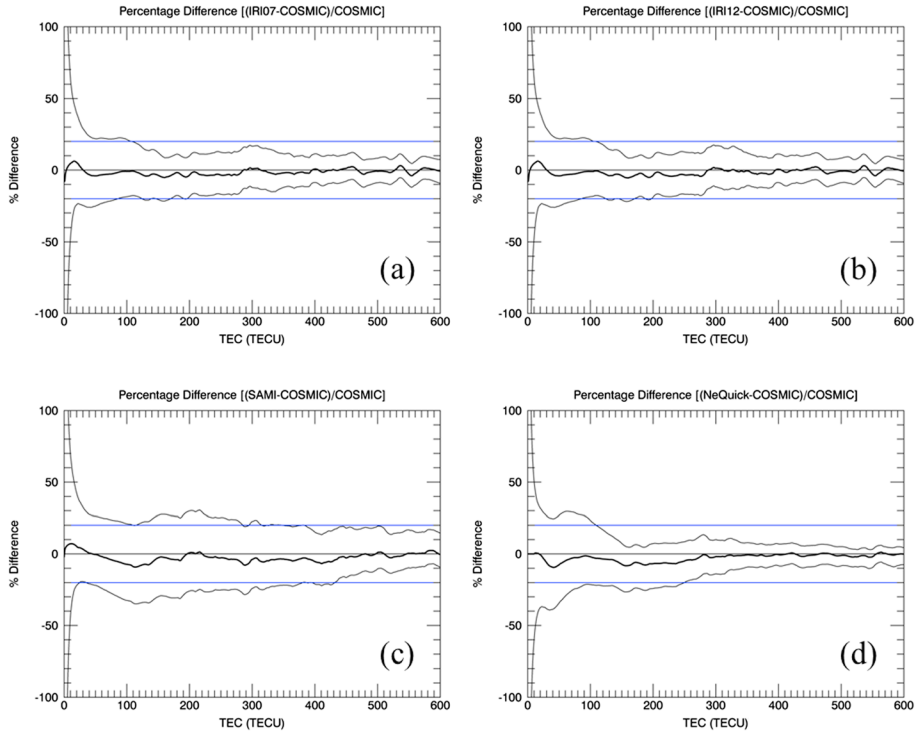

Figure 9. The percentage difference plots derived from the scatterplots in Figure 7. The heavy black line indicates the mode of the distribution at each column across the image. The thinner black lines indicate the upper standard deviation and the lower standard deviation, as the distributions are asymmetric, while the blue horizontal lines indicate 20% difference. (a) IRI-2007, (b) IRI-2012, (c) SAMI-3, and (d) NeQuick. The widths of the distributions are larger than those produced by GAIM, although the performance of NeQuick approaches that of GAIM at TECs $>$ 300 TECU.

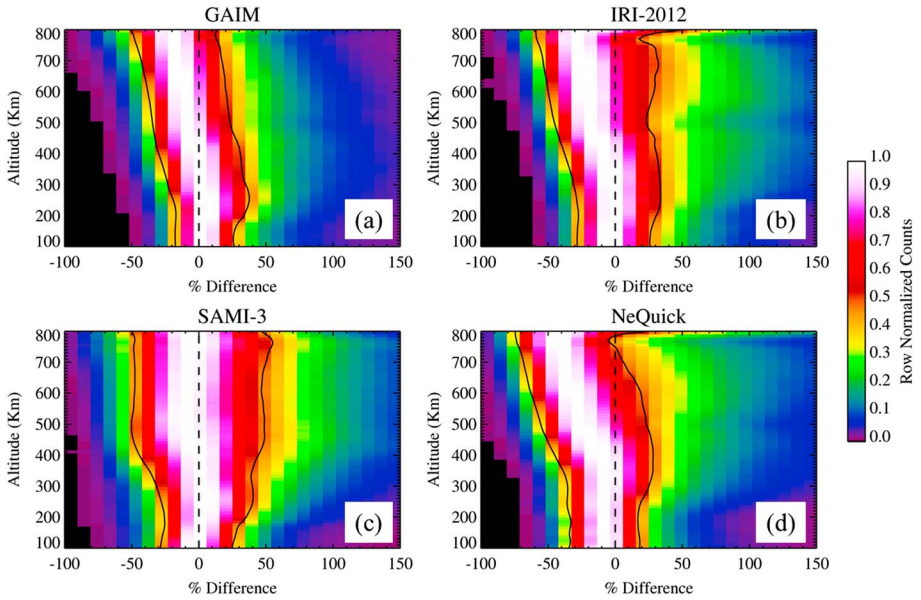

Figure 10. Scatterplots showing the performance of the models as a function of altitude. (a) GAIM, (b) IRI-2012, (c) SAMI-3, and (d) NeQuick. The black lines indicate the half width at half maximum of the distributions. The vertical dashed line indicates perfect agreement between the models and the COSMIC measurements. All four models are underestimating the topside plasma distribution.

shows images of the mean percentage difference between the COSMIC and model TECs as a function of altitude. The dashed vertical lines in the panels indicate a difference of zero, indicating perfect agreement, while the solid black curves indicate the half width at half maximum of the distributions. All of the models are underestimating the TEC in the topside by 15%, 5%, 25%, 25%, and 40%, for GAIM, SAMI-3, IRI-2007, IRI-2012, and NeQuick, respectively. This indicates either that all of the models are not capturing the overall thermodynamic state of the ionosphere, as the topside density is driven largely by the plasma temperature, or that the H^+ and He^+ ion densities are being underestimated. SAMI-3 does the best job, however, which is not surprising as it is a full-physics model that captures both the thermodynamic state of the coupled ionosphere-thermosphere system and also models light ion production and transport. Subsequent to this study, the GAIM-GM model, used in this study, had its vertical correlation length increased to be able to better ingest UV limb radiances from the DMSP satellites; this change might cause GAIM to perform better in the topside ionosphere. We also note that the version of the NeQuick model used in this work was from a 2002 release (ITU-R); subsequent work has ensued on NeQuick with particular attention paid improving model performance [*Coïsson et al.*, 2006; *Leitinger et al.*, 2005; *Nava et al.*, 2008]. We note that the ionospheric slab thickness is defined as the ratio of the vertical TEC to the peak electron density. In an alpha Chapman layer, this slab thickness can be directly related to the *F* region scale height [*Wright*, 1960]. Since the models usually perform well in validations against vertical TEC and either the topside scale height or the light ion densities are too low, our work suggests that the peak density at the *F* region peak may be overestimated by the models or that the ionospheric plasma distribution may be changed in other ways to compensate.

Figure 11 shows maps of the mean percentage difference between the COSMIC and model TECs, analogous to Figure 6. All four models are showing poor performance in the region of the equatorial ionization anomaly and over the South Atlantic Ocean in the area of the Weddell Sea. This is not surprising as there are few ground-based data sources in the regions available for fitting in the empirical models. More problematic is the N-S asymmetry present in all of the maps. The scatterplots presented earlier showed increased scatter but overall showed performance that was quite good. However, the maps reveal a different picture. The overall good agreement of the averages is somewhat fortuitous as demonstrated by the N-S asymmetries.

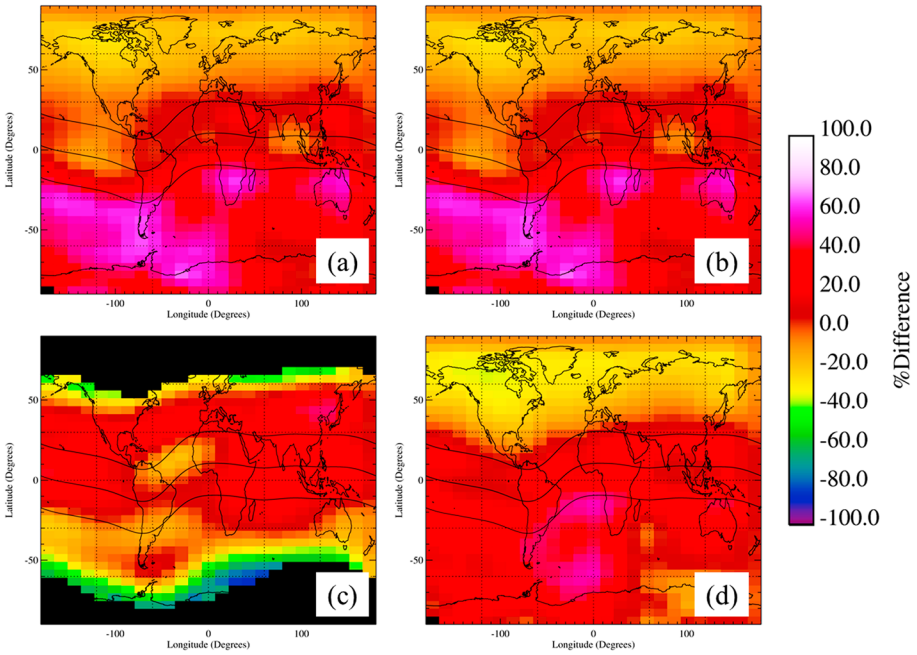

Figure 11. The mean percentage difference between the model TEC and the COSMIC TEC. (a) IRI-2007, (b) IRI-2012, (c) SAMI-3, and (d) NeQuick. The averaging is over all local times and over the 47 day study period. Note that the largest errors are near the magnetic equator (black curve) and in the South Atlantic Ocean in the Weddell Sea anomaly. Both regions lie mostly over open ocean where there are few ground-based data sources upon which to base the empirical models. All four models show a strong N-S asymmetry. SAMI-3 was driven by the empirical Scherliess-Fejer drift model [*Scherliess and Fejer*, 1999], and this climatology may not be adequately capturing the vertical drift.

4. Summary

We showed that the ionospheric models used in this study performed well against COSMIC slant TEC measurements. To focus our study on the ionosphere, we carried out most of the comparisons against PCTEC, where the TEC of the 0° elevation line of sight in each occultation was subtracted from other lines of sight in the occultation. The GAIM model performed the best of all of the models with a negligible additive bias and a multiplicative bias of 0.99. However, the scatter between the measurements and the models is problematic, as it is likely due to space weather that is not well captured by the models. For the GAIM model, which had the lowest scatter of the models, this is 15% full width at half maximum or a 1σ error of 15 TECU at a slant TEC of 100 TECU. Part of this scatter was due to a combination of data-poor regions and poor topside performance. All of the models underestimated the topside scale height or the light ion densities, which can lead to vertical TEC and n_mF_2 errors. This error might be mitigated by tuning the solar and geophysical parameters used to drive the models.

We note that the present study was primarily performed during spring and early summer of 2012 (5 May to 20 June 2012), while the SAMI-3 part of the study was performed for the late fall and early winter of 2011 (1 October 2011 to 31 December 2011). It would be worthwhile to extend a study like ours to cover a longer time period of at least 1 year duration to assess how seasonal effects are captured by the models. Additionally, comparisons of model performance as functions of solar and geomagnetic activity would also be of use.

All of the models tested would be good candidates for inclusion in an ensemble Kalman filter modeling approach. But as the GAIM comparisons showed, additional data sources for ingestion would also help improve ionospheric specification capability and performance. It is also likely that the inclusion of additional data sources would also reduce some of the specification error seen as scatter in our analysis as this is likely due to space weather that is occurring on more regional scales that are not well captured by current ionospheric models.

For example, the wave 4 pattern [*Immel et al.*, 2006] that is the subject of much recent ionospheric research is not well captured by any current model.

Acknowledgments

The Chief of Naval Research supported this work through the Naval Research Laboratory (NRL) 6.1 Base Program. The NeQuick model was obtained via http://www.itu.int/dms_pub/itu-r/oth/0A/04/R0A040000180001ZIPE.zip (17 June 2016). The IRI-2007 and IRI-2012 models were obtained from http://irimodel.org/IRI-2007/ (17 June 2016) and http://iri-model.org/IRI-2012/ (17 June 2016).

References

Anthes, R. A., et al. (2008), The COSMIC/FORMOSAT-3 mission: Early results, *Bull. Am. Meteorol. Soc.*, *89*, 313–333, doi:10.1175/BAMS-89-3-313.

Bilitza, D. (2001), International Reference Ionosphere 2000, *Radio Sci.*, *36*(2), 261–275, doi:10.1029/2000RS002432.

Bilitza, D., and B. W. Reinisch (2008), International Reference Ionosphere 2007: Improvements and new parameters, *Adv. Space Res.*, *42*, 599–609, doi:10.1016/j.asr.2007.07.048.

Bilitza, D., et al. (2014), The International Reference Ionosphere 2012—A model of international collaboration, *J. Space Weather Space Clim.*, *4*, 1–12, doi:10.1051/swsc/2014004.

Catmull, E., and R. Rom (1974), A class of local interpolating splines, in *Computer Aided Geometric Design*, edited by R. E. Barnhill and R. F. Reisenfeld, pp. 317–326, Academic Press, New York.

Coïsson, P., S. M. Radicella, R. Leitinger, and B. Nava (2006), Topside electron density in IRI and NeQuick: Features and limitations, *Adv. Space Res.*, *37*, 937–942.

Di Giovanni, G., and S. R. Radicella (1990), An analytical model of the electron density profile in the ionosphere, *Adv. Space Res.*, *10*, 27–30.

Drob, D. P., et al. (2008), An empirical model of the Earth's horizontal wind fields: HWM07, *J. Geophys. Res.*, *113*, A12304, doi:10.1029/2008JA013668.

Emmert, J. T., D. P. Drob, G. G. Shepherd, G. Hernandez, M. J. Jarvis, J. W. Meriwether, R. J. Niciejewski, D. P. Sipler, and C. A. Tepley (2008), DWM07 global empirical model of upper thermospheric storm-induced disturbance winds, *J. Geophys. Res.*, *113*, A11319, doi:10.1029/2008JA013541.

Huba, J. D., G. Joyce, and J. A. Fedder (2000), Sami2 is Another Model of the Ionosphere (SAMI2): A new low-latitude ionosphere model, *J. Geophys. Res.*, *105*, 23,035, doi:10.1029/2000JA000035.

Huba, J. D., G. Joyce, and J. Krall (2008), Three-dimensional equatorial spread *F* modeling, *Geophys. Res. Lett.*, *35*, L10102, doi:10.1029/2008GL033509.

Immel, T. J., E. Sagawa, S. L. England, S. B. Henderson, M. E. Hagan, S. B. Mende, H. U. Frey, C. M. Swenson, and L. J. Paxton (2006), Control of equatorial ionospheric morphology by atmospheric tides, *Geophys. Res. Lett.*, *33*, L15108, doi:10.1029/2006GL026161.

Lean, J. L., T. N. Woods, F. G. Eparvier, R. R. Meier, D. J. Strickland, J. T. Correira, and J. S. Evans (2011), Solar extreme ultraviolet irradiance: Present, past, and future, *J. Geophys. Res.*, *116*, A01102, doi:10.1029/2010JA015901.

Leitinger, R., M. L. Zhang, and S. M. Radicella (2005), An improved bottomside for the ionospheric electron density model NeQuick, *Ann. of Geophys.*, *48*(3), 525–534.

McDonald, S. E., L. J. Lean, J. D. Huba, G. Joyce, J. T. Emmert, and D. P. Drob (2014), *Long-Term Simulations of the Ionosphere Using SAMI3, Modeling the Ionosphere-Thermosphere System*, *Geophys. Monogr. Ser.*, vol. 201, edited by J. D. Huba, R. Schunk, and G. Khazanov, AGU, Washington, D. C.

Nava, B., P. Coïsson, and S. M. Radicella (2008), A new version of the NeQuick ionosphere electron density model, *J. Atm. and Sol.-Terr. Phys.*, *70*, 1856–1862.

Picone, J. M., A. E. Hedin, D. P. Drob, and A. C. Aikin (2002), NRLMSISE-00 empirical model of the atmosphere: Statistical comparisons and scientific issues, *J. Geophys. Res.*, *107*(A12), 1468, doi:10.1029/2002JA009430.

Radicella, S. M., and M.-L. Zhang (1995), The improved DGR analytical model of electron density height profile and total electron content in the ionosphere, *A. Geofisica*, *38*, 35–41.

Scherliess, L., and B. G. Fejer (1999), Radar and satellite global equatorial F region vertical drift model, *J. Geophys. Res.*, *104*(A4), 6829–6842, doi:10.1029/1999JA900025.

Scherliess, L., et al. (2006), Utah State University Global Assimilation of Ionospheric Measurements Gauss-Markov Kalman filter model of the ionosphere: Model description and validation, *J. Geophys. Res.*, *111*, A11315, doi:10.1029/2006JA011712.

Scherliess, L., D. C. Thompson, and R. W. Schunk (2009), Ionospheric dynamics and drivers obtained from a physics-based data assimilation model, *Radio Sci.*, *44*, RS0A32, doi:10.1029/2008RS004068.

Schunk, R. W., et al. (2004), Global Assimilation of Ionospheric Measurements (GAIM), *Radio Sci.*, *39*, RS1S02, doi:10.1029/2002RS002794.

Wright, J. W. (1960), A model of the *F*-region above $h_{max}F_2$, *J. Geophys. Res.*, *65*, 185, doi:10.1029/JZ065i001p00185.

Yue, X., W. S. Schreiner, Y. C. Lin, C. Rocken, Y. H. Kuo, and B. Zhao (2011a), Data assimilation retrieval of electron density profiles from radio occultation measurements, *J. Geophys. Res.*, *116*, A03317, doi:10.1029/2010JA015980.

Yue, X., W. S. Schreiner, D. Hunt, C. Rocken, and Y. H. Kuo (2011b), Quantitative evaluation of the low Earth orbit satellite based slant total electron content determination, *Space Weather*, *9*, S09001, doi:10.1029/2011SW000687.

Yue, X., et al. (2012), Global 3-D ionospheric electron density reanalysis based on multisource data assimilation, *J. Geophys. Res.*, *117*, A09325, doi:10.1029/2012JA017968.